Available online at www.sciencedirect.com

ScienceDirect

IFAC PapersOnline CONFERENCE PAPER ARCHIVE

IFAC PapersOnLine 52-26 (2019) 255–261

Optimal Experimental Design for a Bistable Gene Regulatory Network

Nathan Braniff, Addison Richards, Brian Ingalls*

*Department of Applied Mathematics, University of Waterloo, Waterloo, Ontario, Canada (*e-mail: bingalls@uwaterloo.ca)*

Abstract: Accurate model calibration is essential for model-based design of synthetic gene regulatory networks. Optimal experimental design (OED) techniques can be used to efficiently decrease parameter uncertainty. However, many biological networks of interest exhibit multimodal response functions due to multistability. These models are incompatible with traditional OED approaches that have been developed for models with mono-modal error distributions. In this work we propose an OED approach for a gene expression model that exhibits bistability via a saddle-node bifurcation with respect to an experimental input. We demonstrate construction of an approximate likelihood and derive the corresponding Fisher information across the monostable and bistable regimes. We use the linear noise approximation for the local error model and apply logistic regression to capture the switching probabilities between the stable equilibria. We then use this Fisher information matrix to generate locally optimal experimental designs for this system. This leads to a simple, qualitative approach to optimal experimental design based on experimental detection of bimodality.

Keywords: Synthetic Biology, Gene Regulatory Networks, Parameter Estimation, Optimal Experimental Design, Stochastic Models, Bistability, Bifurcation

1. INTRODUCTION

Many synthetic biology projects aim to construct designer gene regulatory circuits. These circuits often involve feedback and nonlinear dynamics, including bifurcations and multistability (Del Vecchio et al., 2016). Model-based design can be a critical tool in the development of such systems. However, biological models have traditionally suffered from sloppy parameter estimates and poor predictive accuracy, limiting the effectiveness of modeling in biological design (Erguler and Stumpf, 2011; Gutenkunst et al., 2007).

Optimal experimental design (OED) provides tools by which synthetic biologists can improve the efficiency of precise model calibration (Braniff and Ingalls, 2018; Chakrabarty et al., 2013). However, OED approaches have traditionally been applied to monostable systems, which exhibit monomodal error distributions (Ruess et al., 2015) that are often assumed to be Gaussian (Apgar et al., 2010; Hagen et al., 2013). Many synthetic regulatory systems of interest exhibit bifurcations and multistability (Del Vecchio et al., 2016), which can result in multimodal error distributions. Limited attention has been given to these more complex error distributions in the OED literature. Examples have been developed for linear models (Atkinson and Fedorov, 2001), but they are not directly applicable for modelling biological systems.

In this work we develop an OED procedure for characterizing expression of an inducible auto-activating gene that exhibits bistability over a subset of its induction range. We use a stochastic model to account for random jumping between the two equilibria in the multistable regime. This jumping results in a bimodal error model. We use the linear noise approximation (LNA) to form a Gaussian mixture approximating the multimodal likelihood function. We then apply OED to this approximation, using the Fisher information to identify optimal experiments. Specifically, we identify (i) an optimal set of induction input values, and (ii) the fraction of the overall number of steady-state single-cell observations to be taken at each input. The LNA incurs approximation error when applied to multistable systems (Hortsch and Kremling, 2018). However the LNA is analytically differentiable with respect to both inputs and parameters, and it is computationally tractable, both of which are essential for performing optimization over the experimental space.

Past work has investigated parameter estimation procedures for multistable switches (Otero-Muras et al., 2014) suggesting the tracing of hysteresis loops as a means to detect bistable regions. This procedure requires complex experiments with time-varying inputs and careful consideration of the relaxation timescales as part of the experimental design. Our approach uses a more direct strategy for the identification of bistability, focusing exclusively on steady state observations and bimodality detection. Additionally, we provide a simple procedure for avoiding irregularities caused by bifurcations. We find that, for our example system, the optimal experiments follow a consistent qualitative pattern. Further investigation will address the question of whether this pattern generalizes to a simple heuristic procedure for designing optimal experiments for other bistable systems.

10.1016/j.ifacol.2019.12.267

2. METHODS

We employ a simple one-dimensional model to illustrate the method. Equation 1 depicts the deterministic rate equation for the mean concentration of the protein product x of an auto-activating gene:

$$\frac{d}{dt}x(t) = \alpha_0 + \alpha\frac{(u+x(t))^n}{K^n + (u+x(t))^n} - x(t). \qquad (1)$$

Here, u is the concentration of protein provided via a separate, experimentally inducible, source. We assume u and x are functionally identical, but x can be differentiated during measurement, e.g. via a tag or co-expressed reporter. We take the nominal parameter set as $\alpha_0 = 0.5$ $\alpha = 3$ $K^n = 9$, and $n = 3$. The parameters α_0, α, and K are in arbitrary units of concentration; the time-scale is chosen so the rate of degradation is unity. For this parameterization the deterministic system exhibits bistability for inputs u in the range $u \in [u_L, u_R] = [0.07, 0.22]$, and undergoes saddle-node bifurcations at these points, see Figure 1B. We seek the inputs that provide maximally informative observations for the purpose of accurately estimating the parameter vector $\theta = [\alpha_0, \alpha, K, n]$. We assume the experiments generate a noisy set of observations, $D = [y_1, ..., y_N]$, taken in long-time equilibrium at input values $U = [u_1, ..., u_N]$. Further we assume the observations y_i are measurements of single-cell concentrations (via a high-throughput instrument such as an automated microscope). Below, we derive the distribution of observations y about the mean x and the resulting likelihood function. We use the likelihood to construct the Fisher information matrix (FIM), and use a scalar function of the FIM as our optimization objective, following classic optimal experimental design theory (Fedorov, 2010).

The primary challenge with the proposed approach is that gene expression is noisy, and at long-time equilibrium there will inevitably be jumping between equilibria when the system is operating in the bistable regime. Thus the observations y will be bimodally distributed for inputs $u \in [u_L, u_R]$. We can simulate this jumping behaviour by using the deterministic rate law in equation (1) to construct a corresponding Master equation model, with reaction propensities as follows:

$$\begin{aligned} \text{Production}: &\quad \Omega \cdot \left(\alpha_o + \alpha\frac{(u+\frac{X}{\Omega})^n}{K + (u+\frac{X}{\Omega})^n}\right), \\ \text{Decay}: &\quad X \end{aligned} \qquad (2)$$

Here, X is the discrete (random) protein count and Ω is the system size. Simulating this system using the stochastic simulation algorithm (SSA) at a nominal system size of $\Omega = 90$ (Gillespie, 1977), we see the bimodal distribution for intermediate values of u as shown in Figure 1A.

The bimodal distribution of the observations y cannot be described by normally-distributed homoskedastic or heteroskedastic error models around a single deterministic mean. We instead assume y can be modeled by a Gaussian mixture and propose an approximate log-likelihood for the system of the form:

$$\begin{aligned} \ell(\theta|D,U) = \sum_i \log\{&\rho(u_i)\cdot\varphi_T(y_i|u_i,\theta) \\ &+ [1-\rho(u_i)]\cdot\varphi_B(y_i|u_i,\theta)\} \end{aligned} \qquad (3)$$

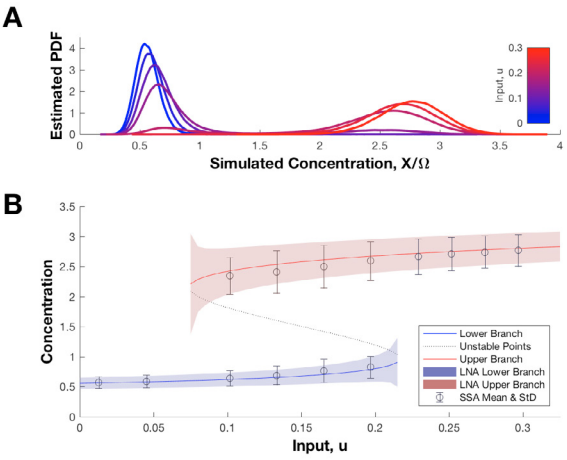

Fig. 1. (A) An empirical density plot of the simulated species concentration X/Ω for various inputs u, simulated using the SSA with $\Omega = 90$. (B) The bifurcation curve (stable, solid; and unstable, dashed) for the steady state protein concentration x^* from the deterministic model, with the LNA-derived standard error (shaded). The simulated mean values (open circles) and standard errors (error bars) were computed from the SSA simulation.

Here $\varphi_T(y_i|u_i,\theta)$ and $\varphi_B(y_i|u_i,\theta)$ are the local distributions of y_i around the top and bottom bifurcation branches, respectively, while ρ represents the probability that a single-cell observation y_i will have originated from $\varphi_T(y_i|u_i,\theta)$ for a given input u_i. Thus $[1-\rho]$ is the probability that the observation originated from $\varphi_B(y_i|u_i,\theta)$

To define $\varphi_T(y_i|u_i,\theta)$ and $\varphi_B(y_i|u_i,\theta)$, we apply Van Kampen's system size expansion (SSE) to the Master equation, using the *ansatz* $X = \Omega x + \sqrt{\Omega}\zeta$, where ζ represents the random fluctuations in species concentration around the deterministic mean concentration x (Van Kampen, 1992). At first order in the SSE, we recover the deterministic rate equation (1) for mean concentration x. At steady state the this rate law yields an equation for the steady state mean x^* in terms of the input u,

$$0 = g(x,u,\theta) = \alpha_0 + \alpha\frac{(u+x)^n}{K^n + (u+x)^n} - x \qquad (4)$$

which has multiple solutions in the bistable region (i.e. for $u \in [u_L, u_R]$). Over that range we denote the lower root (stable fixed point) as x^*_B, the middle root (unstable saddle point) as x^*_M, and the upper root (stable fixed point) as x^*_T. In the monostable region where $u < u_L$, the only root is x^*_B; for $u > u_R$, only x^*_T appears. Thus x^*_B and x^*_T define the bottom and top branches of the bifurcation curve respectively. The stable upper and lower branches are shown in figure 1B along with the means and standard deviations generated from SSA simulations. (To compute the means and standard deviations we used the position relative to the unstable branch to assign each SSA-simulated concentration to either the upper or lower basin of attraction.)

The next order in the SSE yields the linear noise approximation (LNA) (Van Kampen, 1992). From the LNA we have an expression for the local variance of y about x^*;

$$\sigma^2(x^*,u,\theta) = \frac{\left(a_0 + a\frac{(u+x^*)^n}{K^n+(u+x^*)^n} + x\right)}{-2\Omega\frac{\partial}{\partial x}g(x,u,\theta)|_{x=x^*}}, \tag{5}$$

We evaluated this variance function, $\sigma^2(x^*,u,\theta)$, at the roots x_B^* and x_T^* to compute the local variance around each bifurcation branch (Tomioka et al., 2004). Figure 1B shows the reasonable agreement between the SSE and SSA for both the means and the standard deviations, at a system size of $\Omega = 90$. Using the means and variance derived from the SSE we define the local distribution $\varphi_B(y_i|u_i,\theta)$ such that $\{y_i|\rho=0\} \sim \mathcal{N}(x_B^*, \sigma^2(x_B^*,u))$ and $\varphi_T(y_i|u_i,\theta)$ such that $\{y_i|\rho=1\} \sim \mathcal{N}(x_T^*, \sigma^2(x_T^*,u))$.

To describe the branch probability ρ, we use an alternate framing of the system dynamics as stochastic diffusion within a bistable potential. Focusing on the observation y, define $V(y) = \int_{y_0}^{y} -g(\nu,u,\theta)\,d\nu$ as a potential function for the vector field of the deterministic rate equation. Thus, as a somewhat *ad hoc* approximation, we can write $dy(t) = -V(y) + \sqrt{2\epsilon}dW$. Here ϵ represents the strength of a constant noise source and dW are increments from the Wiener process. This approximation does not correspond directly to either the linear noise approximation (which has a constant noise source at steady state but a monostable potential about the deterministic mean) or the Kramers-Moyal expansion (which has a nonlinear diffusion term). However, it allows us to use Kramers' expression for the the escape times between two wells in a potential (Berglund, 2011);

$$\begin{aligned}\tau_{BT} &\approx \frac{2\pi}{\sqrt{V''(x_B^*)|V''(x_M^*)|}} e^{2(|V(x_M^*)-V(x_B^*)|)/\epsilon_B},\\ \tau_{TB} &\approx \frac{2\pi}{\sqrt{V''(x_T^*)|V''(x_M^*)|}} e^{2(|V(x_M^*)-V(x_T^*)|)/\epsilon_T}.\end{aligned} \tag{6}$$

Here τ_{BT} and τ_{TB} are the expected waiting times for the first crossing of the unstable equilibria x_M^* from the bottom-to-top, or top-to-bottom respectively, assuming the system is initialized at equilibrium in the corresponding potential basin. Here ϵ_B and ϵ_T represent the noise strength within each potential. Assuming that the well-to-well transition rates are inversely proportional to these expected waiting times, we can write an equilibrium constant for switching between wells as $K_e = \tau_{BT}/\tau_{TB}$. Recall that we defined ρ as the probability of being in the well around x_T^*. We can then write $\rho = K_e/(1+K_e)$, i.e.

$$\begin{aligned}\rho(u,\theta) \approx \text{logistic}\Big(&\frac{|V(x_M^*)-V(x_B^*)|}{\epsilon_B} - \frac{|V(x_M^*)-V(x_T^*)|}{\epsilon_T}\\ &+ \frac{1}{2}\log\left(V''(x_T^*)\right) - \frac{1}{2}\log\left(V''(x_B^*)\right)\Big),\end{aligned} \tag{7}$$

where $\text{logistic}(z) = (1+e^{-z})^{-1}$. This is essentially the Erying-Kramers (EK) law for reaction rates (Berglund, 2011), where the logistic argument involving the potential is a function of the input u. While this *ad hoc* approximation provides some mathematical insight, we cannot hope to generalize it directly to higher dimensional systems for which potentials cannot be readily constructed. Moreover, it relies on the assumption of constant noise that is small relative to the depth of the potential well. While these drawbacks make this expression unsuitable for direct application, the functional form of the EK approximation for $\rho(u,\theta)$ suggests a logistic function may provide a satisfactory approximation for the branch probability. As such we have used the approximation:

$$\rho(u,c_0,c_1) \approx \frac{1}{1+\exp(-(c_0+c_1u))} \tag{8}$$

Here, the nonlinear expression involving the potential has been replaced with a linear expression in u. To assess the accuracy of this approach, we used the SSA to numerically determine the probability that the state lies in the basin of attraction of either the top or bottom stable fixed points after long simulation times, see figure 2A. As shown, the

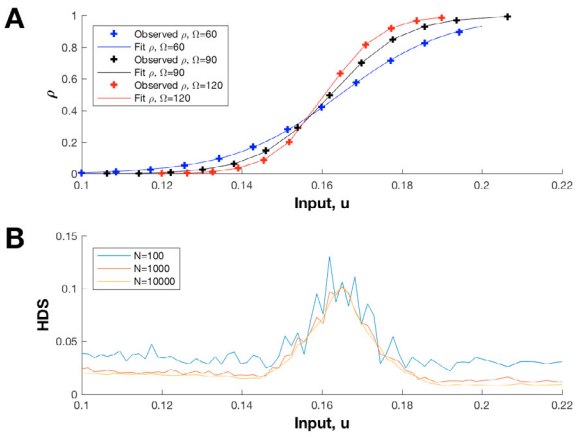

Fig. 2. (A) Probability that the system is within the basin of attraction of the upper equilibrium point in long-time equilibrium for $\Omega = \{60, 90, 120\}$; SSA (circles), corresponding logistic fit (curve). The fit values are; $c = [-18.1\ 111.7]$ for $\Omega = 90$, $c = [-24.2\ 150.3]$ for $\Omega = 120$ and $c = [-12.1\ 73.8]$ for $\Omega = 60$. (B) The Hartigan dip statistic computed for various inputs using $N = 100$, 1000, or 10000 observations. The algorithm was taken from (Mechler et al., 2019).

SSA results are fit well by a logistic function, over a range of system sizes. These logistic curves are specified by parameters c_0, c_1, which we organize into vector $c = [c_0\ \ c_1]$. These are *auxiliary* parameters, in the sense that, while having some underlying connection to mechanistic parameters θ, they are not the direct target of our experiment, and serve primarily to account for variability that would otherwise make the model intractable.

Substituting the expression for $\rho(u,c)$ into (3) results in an appropriate mixture likelihood function on the bistable region. However, it cannot be evaluated as written on the monostable branches, where only one of the two distributions is defined. One approach to resolve this issue would be to modify the behaviour of ρ at the bifurcation points in a piecewise fashion. But that would introduce points of non-differentiability (with respect to θ) in ρ, which would invalidate use of the Fisher information (Pronzato and Pázman, 2013). As a tractable alternative, we define a guaranteed bistability region, as follows. We presume that preliminary experiments have identified a region of bimodality. This can be achieved by, e.g. a screening experiment, using a grid or bisection search with a bimodality statistic, such as the the Hartigan Dip Statistic (HDS) (Hartigan et al., 1985), shown in Figure 2B. (The HDS is a min-max, non-parametric comparison of the

observed distribution with the family of unimodal distributions, see (Hartigan et al., 1985) for details.) The HDS can detect a subinterval of the bistable region where ρ deviates significantly from 0 or 1. Using an appropriate threshold, this data can be used to define a region of guaranteed bistabilty $u \in [B_L, B_R] \subset [u_L, u_R]$. For values of u outside $[B_L, B_R]$, we set ρ to either 0 or 1, thus approximating the system as monostable. By imposing the conservative bounds B_L and B_R, we have traded precision at the bifurcation points for tractability (and smoothness with respect to the parameters) of the resulting likelihood. To make use of this construction we restrict the permissible parameter vectors θ so that model's bifurcation points fall outside the guaranteed bistable interval: $\Theta \in \{\theta | u_L(\theta) < B_L \ \& \ B_R < u_R(\theta)\}$. The likelihood function can then be written as:

$$\begin{aligned}\ell(\theta, c|D, U) = &\sum_i \log\{\rho(u_i, c) \cdot \varphi_T(y_i|u_i, \theta) \\ &+ [1 - \rho(u_i, c)] \cdot \varphi_B(y_i|u_i, \theta)\}\end{aligned} \tag{9}$$

Where:

$$\rho(u, c) = \begin{cases} 0 & u \le B_L \\ \text{logistic}(c_0 + c_1 u) & B_L < u < B_R \\ 1 & B_R \le u \end{cases}$$

Note that $\rho(u, c)$ depends only on the auxiliary parameters c while the local distributions φ_B and φ_T depend only on the reaction parameters θ.

We will use the Fisher information to quantify experimental optimality and thus identify the optimal set of inputs. The inverse of the Fisher information matrix is equivalent to the asymptotic covariance of the parameter estimates computed using a maximum likelihood estimator (Ford et al., 1989). Calculation of the Fisher information for this nonlinear system relies on a nominal parameterization: $\hat{\theta}$, $\hat{c}$. Consequently our results are only guaranteed to be locally optimal. The initial screening experiments used to define the guaranteed bistability bounds can provide these nominal (preliminary) estimates. The Fisher information for a single sample u_i is;

$$I(u_i|\hat{\theta}, \hat{c}) = E_{y_i}\left[\nabla_{\theta,c}\ell(\theta, c|y_i, u_i)^T \nabla_{\theta,c}\ell(\theta, c|y_i, u_i)\right] \tag{10}$$

where y_i is the observed steady state protein concentration resulting from input u_i. For inputs where the response is approximated as monostable (i.e. $u_i < B_L$ or $B_R < u_i$), the Fisher information has an analytic expression. It can be computed as

$$\begin{aligned}I(u_i|\hat{\theta}) = &\frac{\nabla_\theta x^*(u_i, \hat{\theta})^T \nabla_\theta x^*(u_i, \hat{\theta})}{\sigma^2(x^*, u_i, \hat{\theta})} \\ &+ \frac{1}{2}\frac{\left(\nabla_\theta \sigma^2(x^*, u_i, \hat{\theta})^T \nabla_\theta \sigma^2(x^*, u_i, \hat{\theta})\right)}{(\sigma^2(x^*, u_i, \hat{\theta}))^2}\end{aligned} \tag{11}$$

Here x^* correspond to x_B^* or x_T^* depending on the input. The sensitivity of the branch mean x^* is

$$\nabla_\theta x^*(u_i, \theta) = \frac{\frac{\partial g(x^*, u_i, \theta)}{\partial \theta}}{\left(1 - \frac{\partial g(x^*, u_i, \theta)}{\partial x^*}\right)}, \tag{12}$$

For the variances, we can compute the derivatives analytically as

$$\begin{aligned}\nabla_\theta \sigma^2(x^*, u_i, \theta) = &\frac{\partial \sigma^2(x^*, u_i, \theta)}{\partial \theta} \\ &+ \frac{\partial \sigma^2(x^*, u_i, \theta)}{\partial x^*} \nabla_\theta x^*(x^*, u_i, \theta).\end{aligned} \tag{13}$$

To evaluate each of eq. 11-13, we solve for the roots of $g(x^*, u_i, \theta)$, x_B^* and x_T^*, numerically.

For inputs in the guaranteed bistable region $u \in [B_L, B_R]$, calculation of the Fisher information is more complicated due to the mixed Gaussian response. We computed the sensitivity $\nabla_{\theta,c} l(\theta, c|y_i, u_i)$ using the algorithmic differentiation capabilities of CasADi (Andersson et al., 2018). The expectation integral in the Fisher information (equation 10) is then computed numerically using MATLAB's globally adaptive quadrature function `integral`.

In this work we solve for what is known in the OED literature as the approximate optimal design (Pronzato, 2008). Using this approach the optimal design consists of a set of unique inputs $\bar{U} = \{u_1, ..., u_S\}$ and a corresponding set of sampling weights, $\bar{\xi} = \{\xi_1, ..., \xi_S\}$, such that $\sum_i \xi_i = 1$. The weight ξ_i reflects the fraction of the total number of observations that should be made with the given input u_i. (The reason these designs are called approximate is that, with a finite number of total samples in the experiment, one may only approximate the optimal weighting unless the solution happens to have relatively simple fractional weights.) The total Fisher information for the experiment is additive over inputs u (assuming uncorrelated observations), therefore for an approximate design the total FIM is a weighted average, with weights $\bar{\xi} = [\xi_1, ..., \xi_S]$:

$$I_{Tot}(\bar{U}, \bar{\xi}|\hat{\theta}, \hat{c}) = \sum_i^S \xi_i I(u_i|\hat{\theta}, \hat{c}). \tag{14}$$

Next, we select a scalar function of the total information matrix as the OED objective. We use two different optimality measures. The first is the standard D-optimal objective, defined as the determinant of the total Fisher information $|I_{Tot}(\bar{U}|\hat{\theta}, \hat{c})|$ (Atkinson and Donev, 1992). Maximizing this objective is equivalent to minimizing the volume of the asymptotic confidence ellipsoid for the entire parameter set (θ, c). Because our primary interest is in accurately estimating the reaction parameters θ, we also consider D_s-optimality, which aims to specifically minimize the confidence ellipsoid of θ, without consideration for the accuracy in c (Atkinson and Donev, 1992). To define D_s-optimality, first recall that the asymptotic covariance matrix, C, is equal to the inverse of the total FIM, I_{Tot}. We block partition both matrices as follows;

$$I_{Tot} = \begin{bmatrix} I_{\theta,\theta} & I_{\theta,c} \\ I_{\theta,c}^T & I_{c,c} \end{bmatrix}, \ C = \begin{bmatrix} C_{\theta,\theta} & C_{\theta,c} \\ C_{\theta,c}^T & C_{c,c} \end{bmatrix}, \tag{15}$$

A D_s-optimal design minimizes the determinant of $C_{\theta,\theta}$, thus minimizing the confidence ellipsoid for θ. This is equivalent to maximizing the determinant (Atkinson and Donev, 1992):

$$|I_{\theta,\theta} - I_{\theta,c} I_{c,c}^{-1} I_{\theta,c}^T| = \frac{|I_{Tot}|}{|I_{c,c}|}. \tag{16}$$

Having defined the D-optimal and D_s-optimal objectives, we can identify optimal experimental designs $\{\xi_i, u_i\}$. To determine the D-optimal designs we use the CVX package over an adaptively refined grid of candidate u_i's (Grant

and Boyd, 2019). For the D_s-optimal designs we use CasADi and the IPOPT package for optimization, again using an adaptive grid for u (Andersson et al., 2018; Wächter and Biegler, 2006).

3. RESULTS

We begin by investigating the manner in which the optimal designs depend on the nominal values of the logistic parameters c, with θ fixed at the nominal vector $[0.5, 3, \sqrt[3]{9}, 3]$, and with $\Omega = 90$, $B_L = 0.1$ and $B_R = 0.2$. For this analysis, we reparameterize the function ρ such that $c_0 = -c_c c_1$. The new parameter c_c corresponds to the u-value for which $\rho = 0.5$. This allows us to independently set the midpoint and slope of the logistic. Figure 3A depicts ρ for c_1 fixed and c_c varying; Figure 3B shows ρ for varying c_1 values with c_c constant. The parameter ranges were chosen centered on the fit values of $c = [-18,\ 111]$ at $\Omega = 90$ (shown in figure 2A). The corresponding optimal designs are depicted beneath: optimal inputs, u_i (stem locations); optimal weights, ξ_i (stem height). Both the D_s and D optimal designs are shown.

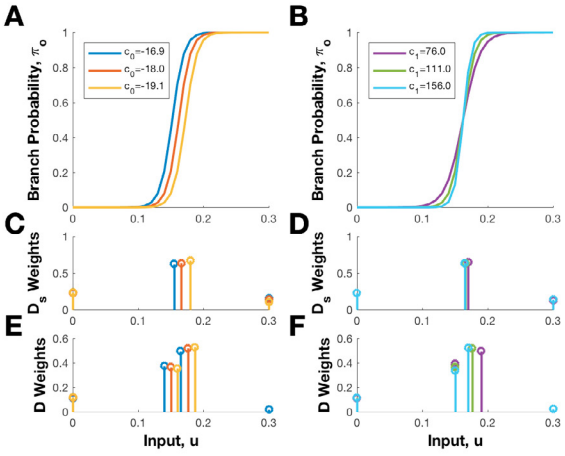

Fig. 3. (A) Plots of ρ for $c_c = 0.152,\ 0.162,\ 0.172$ ($c_0 = -16.9, -18.0, -19.1$), with $c_1 = 111$. (B) Plots of ρ for $c_1 = 76,\ 111,\ 156$ with $c_c = 0.162$ ($c_0 = -12.33,\ -18.00,\ -25.30$). (C, D) Corresponding D_s-optimal designs. (E, F) Corresponding D-optimal designs. Input values u_i correspond to stem locations. Weights ξ_i correspond to stem heights. Note the short stems at both ends of each feasible input range.

These results reveal that the optimal design in each case involves (i) a modest experimental effort to characterize the monostable response at the extremes of the feasible input range, and (ii) a much heavier sampling within the bistable region. For D_s-optimal experiments, the optimal design clusters the bimodal samples near the mid-point of the logistic function (where $\rho \approx 0.5$). For D-optimal experiments, which aim to characterize the full parameter set (θ, c), optimal samples consistently track a pair of percentiles of ρ above and below the mid-point.

We next investigated the sensitivity of optimal sample placement to the nominal θ vector, by holding the logistic parameters constant at $c = [-18.0,\ 111]$ and randomly selecting ten θ vectors from a normal distribution with mean $[0.5, 3, \sqrt[3]{9}, 3]$ and standard deviations of 10% of the mean values. To ensure all θ were consistent with the assumptions used to derive the likelihood, we rejected parameter sets that did not result in deterministic bistability at $u = B_L - \epsilon$ and $u = B_r + \epsilon$, with $\epsilon = 0.05$, as well as rejecting parameters sets that resulted in bistability at $u = 0$ and $u = 0.3$ (the upper and lower bounds of the feasible range for u). Figure 4A depicts stable branches of the ten random bifurcation curves for the chosen θ parameter sets. Figures 4B and C depict the corresponding D_s-optimal and D-optimal designs respectively. With the logistic parameters

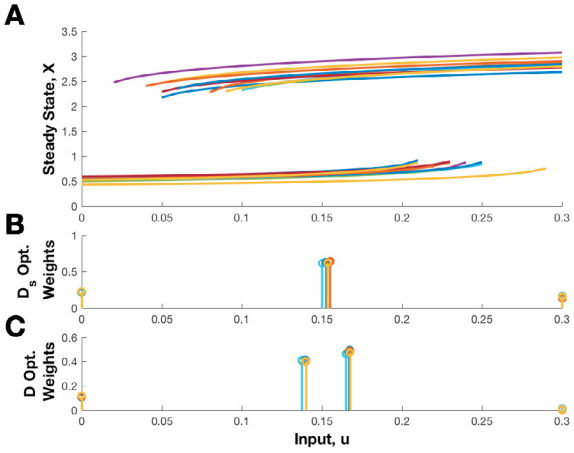

Fig. 4. (A) Stable branches of the bifurcation curves generated from ten random parameter sets θ. (B) D_s-optimal sample weights and inputs for the chosen θ parameters sets, with logistic parameters c held constant. (C) Corresponding D-optimal designs.

held constant, the optimal samples for both D_s and D optimality show a similar placement and weighting, despite the variability in the model parameterization. This finding suggests that, at this systems size ($\Omega = 90$), the shape of the logistic function (which characterizes the bimodality) has a strong effect on the optimal sample placement. These also implies that preference between the D or D_s objectives will depend predominantly on the experimental plans. If the experimenter will only perform a single experiment, the D_s design yields an optimal estimate for the primary parameters θ. However, if the experimenter plans to perform a series of iterated experiments, refining their parameter estimates and re-optimizing their experimental design after each iteration, the D-optimal design will yield a sequence of improved estimates for both θ and c. As the optimal design appears to depend largely on the values of c, the D-optimal objective is ideal for this case.

Referring to Figures 3 and 4, we note that the D_s-optimal designs tended to sample from single mid-point near the middle of the bistable region at a percentile near $\rho = 0.5$. Likewise the D-optimal designs appear to select a pair of optimal inputs that map to relatively consistent and symmetric percentiles on the ρ logistic curve. To further assess this trend, we generated 500 fully randomized parameters sets. Vectors θ was chosen as above; values of c_1 were selected from a uniform distribution over [91 141], while c_c was selected from a uniform distribution over [0.125 0.175]. This ensured the mid-point $\rho = 0.5$ did not fall too close to the boundaries of the guaranteed bistable

region $B_L = 0.1$ and $B_R = 0.2$. Figure 5 shows histograms of the D_s and D-optimal sampling locations in the bistable region across all of the randomly generated parameter sets, where the optimal inputs u have been mapped against percentiles of the logistic ρ. The figure shows clear trends:

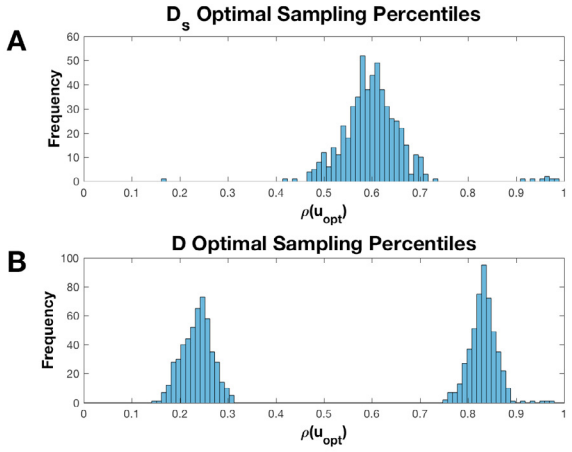

Fig. 5. (A) Histogram for 500 random parameters sets; shown are the frequency of D_s-optimal input values that fall within the bistable region, plotted according to the percentiles of the logistic ρ to which they correspond. (B) Corresponding histogram for D-optimal inputs.

the D_s-optimal input, for use when applying a single round of OED, lies near the 60th percentile of ρ; the D-optimal inputs, which are suited to an iterative OED application, occur near the 25th and 85th percentiles of ρ. Referring to Figure 2, we note that the 60th percentile of ρ is approximately where the HDS peaks, while the 25th and 85th percentiles occur where the HDS rises above the baseline. These results suggest a simple heuristic for performing OED in this bistable system by using the HDS to do a preliminary search for these locations. After these critical values have been located, the experimenter can use the existing data to provide initial estimates of $\hat{\theta}$ and $\hat{c}$ and perform a D or D_s optimal design. For a crude approximation of the optimal design, the logistic could be fit using only the peak and bounds of the elevated HDS signal to approximate the percentile locations. These critical HDS locations could also be used to select the inputs u directly. The sampling weights ξ could then be approximated based on an average of weights across many θ values, as shown in Figure 4. As shown in Figure 4B and C, θ appears to have a limited effect on the optimal design once the logistic is known, with the majority of samples being taken in the biomodal input range.

4. CONCLUSION

In this work we applied OED to an inducible and auto-activating gene expression motif that exhibits bistability. We used a stochastic model to derive an approximate likelihood function, based on the LNA, and a logistic approximation for stochastic switching between stable points motivated by Eyring-Kramers' law. We defined a likelihood to avoid irregularities caused by the bifurcations. We then used D_s and D-optimality criteria to determine optimal inputs and sampling proportions for steady state experiments. We showed that, for the given nominal parameter set and system sizes, the logistic switching function strongly influences the optimal input placement and that optimal inputs roughly correspond to certain percentiles on the logistic curve. Our results suggest that bimodality statistics, like the HDS, may provide a convenient method to perform optimal experiments in the absence of accurate initial estimates for the model parameters. These results can be further investigated by additional simulation studies, to examine a wider range of system sizes and parameters. Additional tests can incorporate maximum likelihood fitting to SSA-generated data. We chose the somewhat artificial one-dimensional system used here because it provided a simple, tractable example, allowing us to more thoroughly illustrate the connection between optimal designs and bistability. Extending our analysis to higher-dimensional systems will reveal whether the simple design heuristic we discovered may be representative of a more general property of OED for bistable systems. An obvious next step is to extend our analysis to a more realistic two-dimensional toggle switch, a direction which we are currently pursuing. Another possible line of inquiry would involve using model and dimensionality reduction techniques to map higher dimensional systems into a one or two dimensional observation space. These reduction techniques may be easier to apply at steady state, rather than in a dynamic context, which is an attractive feature of targeting steady state experiments. Finding an appropriate model reduction procedure would ideally make it straightforward to validate and apply our heuristic design rule to a much broader class of systems.

REFERENCES

Andersson, J.A.E., Gillis, J., Horn, G., Rawlings, J.B., and Diehl, M. (2018). CasADi – A software framework for nonlinear optimization and optimal control. *Mathematical Programming Computation (In Press)*.

Apgar, J.F., Witmer, D.K., White, F.M., and Tidor, B. (2010). Sloppy models, parameter uncertainty, and the role of experimental design. *Molecular BioSystems*, 6(10), 1890–1900.

Atkinson, A. and Donev, A. (1992). *Optimum Experimental Designs*. Oxford University Press.

Atkinson, A.C. and Fedorov, V. (2001). Some history leading to design criteria for bayesian prediction. In *Optimum Design 2000*, 3–14. Springer.

Berglund, N. (2011). Kramers' law: Validity, derivations and generalisations. *arXiv preprint arXiv:1106.5799*.

Braniff, N. and Ingalls, B. (2018). New opportunities for optimal design of dynamic experiments in systems and synthetic biology. *Current Opinion in Systems Biology*.

Chakrabarty, A., Buzzard, G.T., and Rundell, A.E. (2013). Model-based design of experiments for cellular processes. *Wiley Interdisciplinary Reviews: Systems Biology and Medicine*, 5(2), 181–203.

Del Vecchio, D., Dy, A.J., and Qian, Y. (2016). Control theory meets synthetic biology. *Journal of The Royal Society Interface*, 13(120), 20160380.

Erguler, K. and Stumpf, M.P. (2011). Practical limits for reverse engineering of dynamical systems: a statistical analysis of sensitivity and parameter inferability in

systems biology models. *Molecular BioSystems*, 7(5), 1593–1602.

Fedorov, V. (2010). Optimal experimental design. *Wiley Interdisciplinary Reviews: Computational Statistics*, 2(5), 581–589.

Ford, I., Titterington, D., and Kitsos, C.P. (1989). Recent advances in nonlinear experimental design. *Technometrics*, 31(1), 49–60x.

Gillespie, D.T. (1977). Exact stochastic simulation of coupled chemical reactions. *The Journal of Physical Chemistry*, 81(25), 2340–2361.

Grant, M. and Boyd, S. (2019). CVX: Matlab software for disciplined convex programming, version 2.1. `http://cvxr.com/cvx`.

Gutenkunst, R.N., Waterfall, J.J., Casey, F.P., Brown, K.S., Myers, C.R., and Sethna, J.P. (2007). Universally sloppy parameter sensitivities in systems biology models. *PLoS Computational Biology*, 3(10), e189.

Hagen, D.R., White, J.K., and Tidor, B. (2013). Convergence in parameters and predictions using computational experimental design. *Interface Focus*, 3(4), 20130008.

Hartigan, J.A., Hartigan, P.M., et al. (1985). The dip test of unimodality. *The Annals of Statistics*, 13(1), 70–84.

Hortsch, S.K. and Kremling, A. (2018). Characterization of noise in multistable genetic circuits reveals ways to modulate heterogeneity. *PloS one*, 13(3), e0194779.

Mechler, F., Hartigan, J., and Hartigan, P. (2019). Matlab code for hartigan's dip statistic. `http://www.nicprice.net/diptest/`.

Otero-Muras, I., Yordanov, P., and Stelling, J. (2014). A method for inverse bifurcation of biochemical switches: inferring parameters from dose response curves. *BMC Systems Biology*, 8(1), 114.

Pronzato, L. (2008). Optimal experimental design and some related control problems. *Automatica*, 44(2), 303–325.

Pronzato, L. and Pázman, A. (2013). *Design of experiments in nonlinear models*. Springer.

Ruess, J., Parise, F., Milias-Argeitis, A., Khammash, M., and Lygeros, J. (2015). Iterative experiment design guides the characterization of a light-inducible gene expression circuit. *Proceedings of the National Academy of Sciences USA*, 112(26), 8148–8153.

Tomioka, R., Kimura, H., Kobayashi, T.J., and Aihara, K. (2004). Multivariate analysis of noise in genetic regulatory networks. *Journal of Theoretical Biology*, 229(4), 501–521.

Van Kampen, N.G. (1992). *Stochastic processes in physics and chemistry*. Elsevier.

Wächter, A. and Biegler, L.T. (2006). On the implementation of an interior-point filter line-search algorithm for large-scale nonlinear programming. *Mathematical Programming*, 106(1), 25–57.